Journal of Diabetes Science and Technology
Volume 7, Issue 1, January 2013

SYMPOSIUM

Gel Encapsulation of Glucose Nanosensors for Prolonged *In Vivo* Lifetime

Mary K. Balaconis, B.S.,[1] and Heather A. Clark, Ph.D.[2]

Abstract

Background:

Fluorescent glucose-sensitive nanosensors have previously been used *in vivo* to track glucose concentration changes in interstitial fluid. However, this technology was limited because of loss of fluorescence intensity due to particle diffusion from the injection site. In this study, we encapsulated the nanosensors into injectable gels to mitigate nanosensor migration *in vivo*.

Methods:

Glucose-sensitive nanosensors were encapsulated in two different commercially available gelling agents: gel 1 and gel 2. Multiple formulations of each gel were assessed *in vitro* for their nanosensor encapsulation efficiency, permeability to glucose, and nanosensor retention over time. The optimal formulation for each gel, as determined from the *in vitro* assessment, was then tested in mice, and the lifetime of the encapsulated nanosensors was compared with controls of nanosensors without gel.

Results:

Five gel formulations had encapsulation efficiencies of the nanosensors greater than 90%. Additionally, they retained up to 20% and 40% of the nanosensors over 24 h for gel 1 and gel 2, respectively. *In vivo*, both gels prevented diffusion of glucose nanosensors at least three times greater than the controls.

Conclusions:

Encapsulating glucose nanosensors in two injectable gels prolonged nanosensor lifetime *in vivo*; however, the lifetime must still be increased further to be applicable for diabetes monitoring.

J Diabetes Sci Technol 2012;7(1):53–61

Author Affiliations: [1]Department of Bioengineering, Northeastern University, Boston, Massachusetts; and [2]Department of Pharmaceutical Sciences, Northeastern University, Boston, Massachusetts

Abbreviations: (ARS) alizarin red S, (DOS) bis(2-ethylhexyl) sebacate, (PBS) phosphate-buffered saline, (PEG 550) 1,2-distearoyl-*sn*-glycero-3-phosphoethanolamine-N-[methoxy(polyethylene glycol)-550] (ammonium salt) in chloroform, (PVC-COOH) poly(vinyl chloride) carboxylated, (TDMAC) tridodecylmethylammonium chloride, (THF) tetrahydrofuran

Keywords: diabetes, glucose nanosensors, injectable gels, optode

Corresponding Author: Heather A. Clark, Ph.D., Northeastern University, 360 Huntington Ave., Boston, MA 02115; email address h.clark@neu.edu

Introduction

The worldwide prevalence of diabetes has spurred interest in continuous glucose monitoring systems as an alternative to the finger-prick method. Glucose monitors such as DexCom™ STS™ Continuous Glucose Monitoring System and Medtronic's Guardian® REAL-Time Continuous Glucose Monitoring System are commercially available and approved by the Food and Drug Administration to track trends in glucose levels.[1,2] However, further research into novel approaches for glucose monitoring is still of interest in order to prolong sensor lifetimes, improve accuracy, and minimize invasiveness of measurements. Several reviews, such as those written by Wang,[3] Pickup and coauthors,[4] Steiner and coauthors,[5] and Cash and Clark,[6] cover the scope of these developments that include the extension of nanotechnology to glucose sensing. For example, glucose microsensors and nanosensors provide the benefits of rapid response times and ease of implantation due to their large surface-area-to-volume ratio and small size.[6] Chaudhary and coauthors[7] are developing a "smart tattoo" composed of dissolved-core alginate microspheres to be implanted into the skin and monitor glucose levels in interstitial fluid. These sensors use fluorescence resonance energy transfer and a competitive binding mechanism with a noncatalytic mutant of glucose oxidase[8] to repeatedly monitor reversible changes in glucose at physiological levels. In other work, nanosensors using boronic acids as a nonbiological recognition element for glucose have also been investigated because of boronic acids' affinity for 1,2 diols.[5] A common sensing mechanism involving boronic acids is the competitive binding between a fluorescent reporter and glucose for the boronic acid binding site. The fluorescence of the reporter is different in the bound and unbound states, yielding a change in measured signal as the reporter is displaced from the boronic acid. Wang and coauthors[9] developed glucose sensing vesicles using this mechanism with phenylboronic acid, glucose, and the fluorescent reporter alizarin red S (ARS).[9] Alizarin red S was electrostatically coupled to cationic quaternary ammonium salts that self-assembled into vesicles in solution. As glucose was added to the system, ARS was displaced by glucose, which resulted in a decrease in intensity, because the unbound ARS is significantly less fluorescent. Our group utilizes a similar competitive binding scheme as the basis for functional nanosensors, but the sensing components are embedded in a lipophilic, highly plasticized polymeric particle into which glucose is extracted.[10,11] The hydrophobic particle design has several advantages that include isolation of the sensing components from biological fluid to prevent biofouling[12] and tunability of the system to adjust the dynamic range.[13]

Our glucose-sensitive nanosensors successfully tracked changes in glucose levels when injected subcutaneously along the backs of mice.[10] However, the monitoring time was limited to 1 h because of the loss of signal intensity at the injection site. Studies conducted by Gopee and coauthors[14] with intradermally injected quantum dots found that quantum dots migrated from the site of injection, with 60% of quantum dots remaining at the injection site after 24 h. Our nanosensors were implanted similarly in the skin, and migration was assumed to be the main cause of signal loss over time. To mitigate sensor migration in our system, sensor geometry was altered into microworms that limited sensor diffusion and prolonged their lifetime in the skin more than the nanosensors alone.[15] However, the yield of microworms was not sufficient for *in vivo* monitoring. In this study, we encapsulated glucose nanosensors in injectable gels as another approach to prevent nanosensor diffusion *in vivo*. Injectable gels have made an impact in fields such as drug delivery and tissue engineering because they form under mild conditions, are easily implantable, and are biodegradable.[16] These advantages make injectable gels ideal implantation vehicles for the glucose nanosensors. The primary focus of this study was to investigate injectable gels for limiting nanosensor migration *in vivo*. Important characteristics of the glucose sensors such as dynamic range, sensitivity, reversibility, and lifetime have been previously addressed,[10,11] and no work on sensor development is discussed here.

Materials

Matrigel™ basement membrane matrix (gel 1; growth factor reduced, phenol-red-free, lactate-dehydrogenase-elevating-virus-free) and 31 G insulin syringes were purchased from BD Biosciences (Franklin Lakes, NJ). Extracel-X® hydrogel kit (gel 2) was purchased from Glycosan Biosystems Inc. (Alameda, CA). Bis(2-ethylhexyl) sebacate (DOS), tridodecylmethylammonium chloride (TDMAC), alizarin (dye content 97%), tetrahydrofuran (THF; anhydrous, ≥99.9%, inhibitor-free), and chloroform (Chromaslov®, ≥99.8%) were purchased from Sigma-Aldrich (St. Louis, MO).

Octylboronic acid was purchased from Synthonix Inc. (Wake Forest, NC). Gibco® phosphate-buffered saline (PBS) (1x, pH = 7.4) was acquired from Life Technologies (Grand Island, NY) and poly(vinyl chloride) carboxylated (PVC-COOH) was purchased from Scientific Polymer Products Inc. (Ontario, NY). Amicon Ultra centrifugal filters (molecular weight cutoff 100 kDa) were obtained from Millipore (Billerica, MA). 1,2-distearoyl-*sn*-glycero-3-phosphoethanolamine-N-[methoxy(polyethylene glycol)-550] (ammonium salt) in chloroform (PEG 550) was purchased from Avanti Polar Lipids Inc. (Alabaster, AL). SKH1-E mice were purchased from Charles River Laboratories International Inc. (Wilmington, MA).

Methods

Optode Cocktail

Macrosensors and nanosensors were fabricated from an optode cocktail that contained all sensing components: 30 mg of PVC-COOH, 60 µl of DOS, 3 mg of octylboronic acid, 4 mg TDMAC, and 1 mg of alizarin, all dissolved in 500 µl of THF. The selection, optimization, and characterization of these components for glucose sensing are described elsewhere.[10,11]

Nanosensor Fabrication

Fabrication of glucose nanosensors have been described previously.[10] Briefly, the optode cocktail was dried for at least 4 h on a glass plate. It was then removed from the plate and placed into a scintillation vial along with 5 ml of PBS, 5 mg of PEG 550, and 500 µl of total chloroform. The mixture was sonicated using a Branson digital sonifier (Danbury, CT) for 3 min at 40% amplitude. The nanosensors were concentrated using Amicon Ultra centrifugal filters prior to encapsulation in the gelling agents.

Gel Preparation

Two commercially available gels were selected for encapsulating the nanosensors. Each gel has applications in cell encapsulation and tumor growth models.[17,18] Gels were prepared according to the manufacturer's instructions and diluted with nanosensors and PBS according to the ratios in **Tables 1** and **2** to a total volume of 300 µl. The gelling agents were allowed to gel in a 31 G insulin syringe for at least 20 and 90 min for gel 1 and gel 2, respectively. All gels were formed prior to the beginning of experiments. Gel 1 is formed by simply bringing the gel to room temperature. Gel 2 is formed by crosslinking a thiol-modified hyaluronan and thiol-modified gelatin with a thiol-reactive crosslinker, polyethylene glycol diacrylate. For all the gel formulations listed in **Table 2**, hyaluronan and gelatin were used in equal parts and polyethylene glycol diacrylate was 20% of the total gel volume. In the case of both gels, dilution of the gel components with the nanosensors and PBS decreases their stiffness.[18,19] To serve as a control for no gel, nanosensors were diluted with only PBS to a final volume of 300 µl.

Nanosensor Encapsulation Efficiency

Prepared gel (100 µl) with sensors or the no-gel control was injected into a 96-well optical bottom well plate. Fluorescence measurements were acquired on a SpectraMax Gemini EM plate reader (Molecular Devices, Sunnyvale, CA) at 460 and 570 nm for excitation and emission wavelengths, respectively. After the initial reading, the gels were washed

Table 1.
Ratio of Components for Each Gel 1 Formulation[a]

Gel 1: Nanosensors/PBS	Nanosensors	PBS	Gel 1
Control	1	5	0
5:1	1	0	5
2:1	1	1	4
1:1	1	2	3

[a] All gels were made with a total volume of 300 µl.

Table 2.
Ratio of Components for Each Gel 2 Formulation[a]

Gel 2: Nanosensors/PBS	Nanosensors	PBS	Gel 2
Control	1	5	0
5:1	1	0	5
3:1	1	0.5	4.5
2:1	1	1	4

[a] All gels were made with a total volume of 300 µl.

with 100 μl of PBS, the PBS was removed, and then a second measurement was acquired. The encapsulation efficiency was calculated as the fluorescence intensity of the after wash measurement divided by the initial measurement for each sample. This ratio was then expressed as a percentage.

Glucose Permeability through Gels

Glucose macrosensors were used to test glucose permeability because they can be adhered to a surface, eliminating the possibility of unencapsulated nanosensors contributing to sensor response. The macrosensors are formed by pipetting the optode cocktail (2 μl) onto glass discs adhered to the bottom of a 96-well optical bottom well plate and then dried. A total of 200 μl of PBS was added to each well, and the sensors were hydrated in PBS for at least 4 h until their fluorescence intensity stabilized. All fluorescence measurements were acquired at 460 and 570 nm for excitation and emission wavelengths, respectively, using a SpectraMax Gemini EM plate reader. After hydration, 100 μl of gels were injected over the macrosensors and adjusted until they covered the entire bottom of the well plate. Gels were prepared according to the ratios in **Tables 1** and **2**, but the nanosensors were substituted with PBS. For a no-gel control, 100 μl of PBS was substituted for the gels. The concentration of glucose added was dependent upon the gel used and its ratio of dilution such that, for all cases, the final glucose concentration in each well was equal to 9000 mg/dl. The macrosensors and nanosensors have a center of dynamic range of 342 and 684 mg/dl,[10] respectively, but high concentrations of glucose were used here in order to maximize sensor response. Gel 1 is provided in 0.5 mg/dl of glucose Dulbecco's Modified Eagle Medium, and the glucose concentration in each gel 1 formulation was calculated. Gel 2, as provided by the manufacturer, is reconstituted in PBS, and we assumed that 100 μl of gel 2 was equivalent to 100 μl of PBS. The fluorescence response of the macrosensors was monitored for 3 h at 5 min intervals. Fluorescence measurements were normalized to time 0 and then subtracted from the control wells for each gel formulation. This difference was then expressed as a percentage change, and the error bars were calculated using error propagation.

Gel Retention of Nanosensors

Glucose nanosensors were encapsulated in gels as described in the gel preparation section. A total of 40 μl of gel was injected onto a glass bottom petri dish that was then filled with 4 ml of PBS. The gels were placed in an incubator at 37 °C for 10 min and then imaged using an IVIS Lumina II small animal imager (Caliper Life Sciences, Hopkinton, MA). Images were acquired with 465 nm excitation and 580 nm emission filters. They were recorded approximately every half hour for the first 2 h and then at 6.5 h and approximately 24 h. Between measurements, the gels were stored in an incubator at 37 °C. The bulk degradation of the nanosensors (sensor degradation, component leaching, photobleaching) over this time was also monitored to separate these effects from the loss of intensity caused by diffusion. For the bulk degradation controls, 40 μl of glucose nanosensors in PBS was placed in microcentrifuge tubes and imaged at the same time points as mentioned earlier. In between measurements, the nanosensors were stored in an incubator at 37 °C. For analysis, the total radiant efficiency from a region of interest encompassing either the gel or the nanosensors for the bulk degradation control was selected, normalized to the time 0 measurement, and plotted over time to determine the rate of nanosensor diffusion out of the gel.

In Vivo *Testing*

All animal procedures were approved by Northeastern University's Institutional Animal Care and Use Committee. Glucose nanosensors were encapsulated in gels according to the protocol in the gel preparation subsection or diluted with PBS for the no-gel control. SKH1-E mice were anesthetized, and 40 μl of each gel with nanosensors and a no-gel control were injected intradermally along their backs. Intradermal injections were achieved by pinching the skin and then injecting nanosensors with or without gel while the syringe was inserted parallel to the skin. Characteristic of intradermal injections, a bleb or small skin welt was visible after injection.[20] Mice were imaged with an IVIS Lumina II small animal imager with excitation and emission filters at 465 and 580 nm, respectively. Images were acquired for the first 60 min at 10 min intervals, and an additional measurement was taken 3 h post-injection. Similar to the gel retention experiments, the total radiant efficiency from a region of interest surrounding each injection spot was selected for analysis. An additional region of interest with skin only was also selected to determine the background skin fluorescence. The background fluorescence from the skin was subtracted from the region of interest, and the data were normalized to time point 0.

Results

In Vitro *Characterization*

Both gelling systems were assessed for three critical characteristics: encapsulation efficiency, glucose permeability into the gel, and sensor retention over time. Gel formulations were down-selected based on these *in vitro* characteristics prior to *in vivo* testing. First, nanosensors were mixed with gel 1 and gel 2 and diluted at different ratios to adjust gel stiffness. Their encapsulation efficiency of nanosensors is shown in **Figure 1**. All gels encapsulated the nanosensors better than the control, and five out of six gels lost only 10% of their intensity after washing. Gel 1 showed no correlation between stiffness and encapsulation efficiency, whereas the encapsulation efficiency of gel 2 decreased with decreased stiffness. The encapsulation efficiency of gel 2, 2:1, was not downselected in further experiments because of its poor performance compared with the other formulations.

Gel encapsulation of the nanosensors may affect their ability to monitor real-time changes in glucose concentration because of limited-to-no glucose permeability into the gel and potential delays in response. Therefore, glucose permeability into the gels was tested. To determine glucose permeability, glucose macrosensors were used rather than nanosensors to eliminate unencapsulated nanosensors from contributing to the fluorescence response to glucose. Additionally, glucose macrosensors respond over the course of 1 h[10] and thus added to the overall monitoring time required. The percentage change in signal of the glucose macrosensors as a function of time are shown in **Figure 2** for gel 1 and **Figure 3** for gel 2. The gels were permeable to glucose with the response kinetics linear as a function of time until maximum response was achieved. The gel coating caused a delay in sensor response because glucose must diffuse through the entire gel layer before being sensed by the glucose macrosensors. Previous research on glucose diffusion through gels calculate these delays using lag-time analysis, where the delay is the x intercept from a linear fit of total glucose diffusion through the gel membrane over time.[21–23] In the case of our sensors, fluorescence response is related to glucose concentration, and therefore the x intercept of the linear fluorescence response was used for delay calculations. For gel 1, the gel coating caused a lag time for initiating sensor response by 0, 16, and 19 min for the ratios 5:1, 2:1, and 1:1, respectively. Similarly, for gel 2, the response was delayed by 44 and 52 min for the ratios of 5:1 and 3:1, respectively. For both gel 1 and gel 2, variability in sensor response increased with gel stiffness, but all gels in each grouping had a similar percentage change to glucose, and therefore, no downselection was made after this stage. Finally, the assessment of nanosensor retention in the gels was performed. **Figures 4A–C** show the gel 1 ratios with encapsulated nanosensors at four distinct time points. Over 24 h, the fluorescence intensity of the immobilized sensors decreased as the total number of sensors decreased. Sensors diffused away from the edges of the gel but were still retained in the center, as anticipated. **Figure 4D** plots the average total radiant efficiency for each gel ratio over time along with the bulk degradation control. Since bulk degradation of the sensors encompasses sensor degradation, component leaching, and photobleaching, the difference of intensities between the bulk degradation control and gels is assumed to be diffusion of sensors out of the gel. To determine differences in the rate of signal loss between the gels, the data between 0 and 6.5 h were fitted to the exponential model:

$$y = Ae^{R_0 t}$$

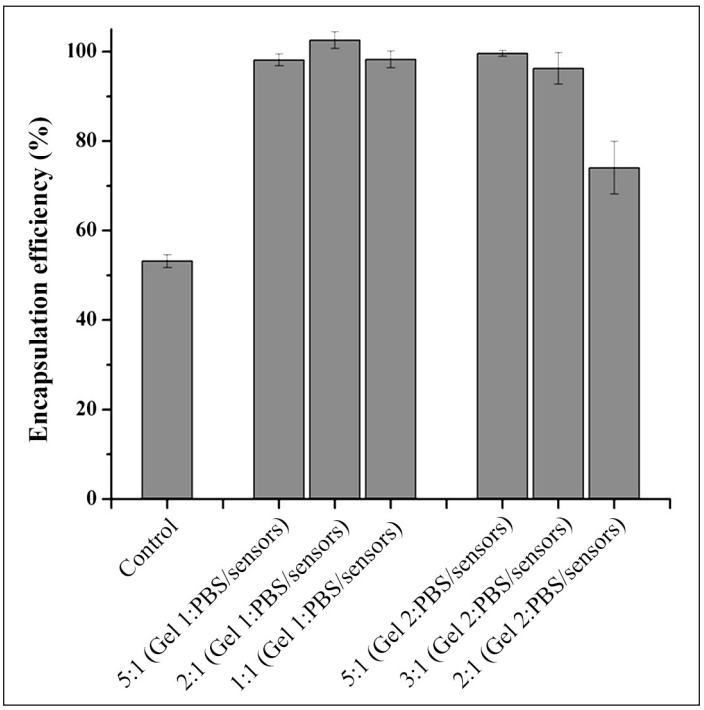

Figure 1. Encapsulation efficiency of gels. Glucose nanosensors were mixed with gelling agents with variable stiffness and allowed to gel. Shown here is the percentage change in fluorescence intensity after the gels were washed with PBS. n = 5 for the control, 2:1 gel 1, and 2:1 gel 2, and n = 6 for 5:1 gel 1, 1:1 gel 1, 5:1 gel 2, and 3:1 gel 2. Error bars represent standard deviations.

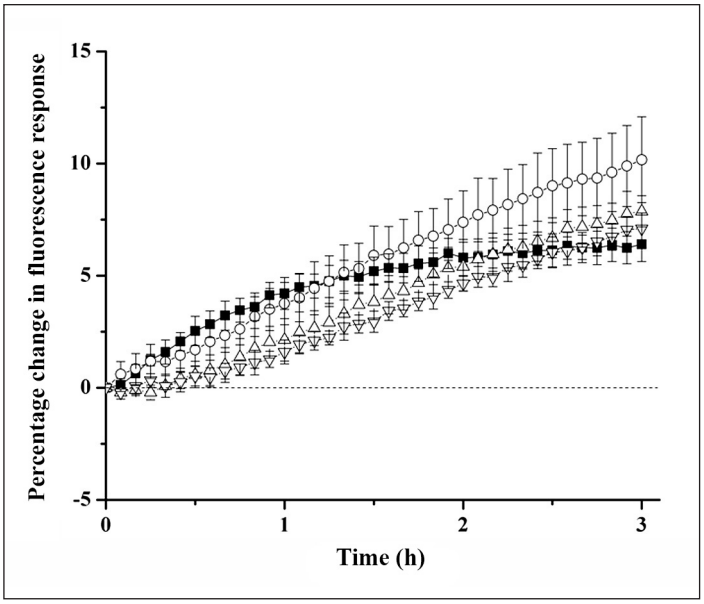

Figure 2. Glucose permeability through gel 1. Glucose macrosensors were layered with different gel 1 formulations of variable stiffness and then exposed to 0 and 9000 g/dl of glucose for the control and experimental groups, respectively. The percentage difference between the controls and experimental groups are plotted against time for no gel (■), 5:1 (gel 1: PBS; ○), 2:1 (gel 1: PBS; △), and 1:1 (gel 1: PBS; ▽). n = 6 for the no-gel control, n = 5 for formulations 5:1 and formulation 2:1, and n = 5 and 4 for the 1:1 formulation experimental and control groups, respectively. Error bars were calculated using error propagation.

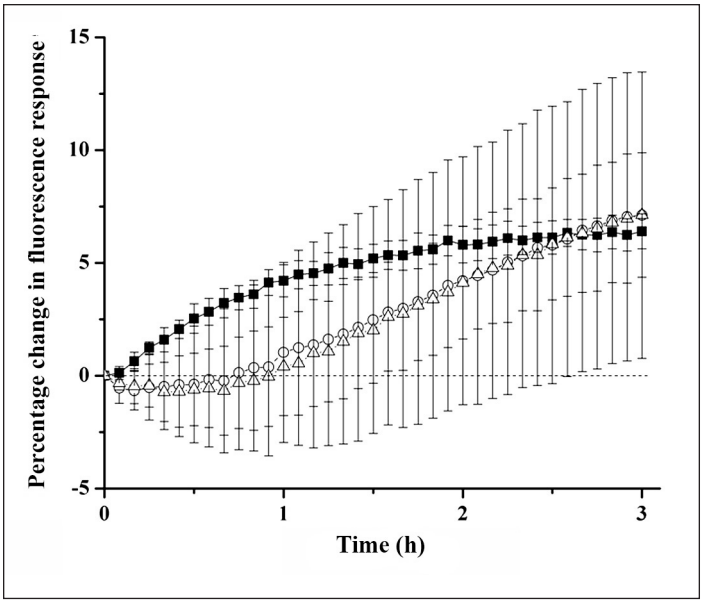

Figure 3. Glucose permeability through gel 2. Glucose macrosensors were layered with different gel 2 formulations of variable stiffness and then exposed to 0 and 9000 g/dl of glucose for the control and experimental groups, respectively. The percentage difference between the controls and experimental groups are plotted against time for no gel (■), 5:1 (gel 2: PBS; ○), and 3:1 (gel 2: PBS; △). n = 6 and 4 for the no-gel control and gel 2, respectively. Error bars were calculated using error propagation.

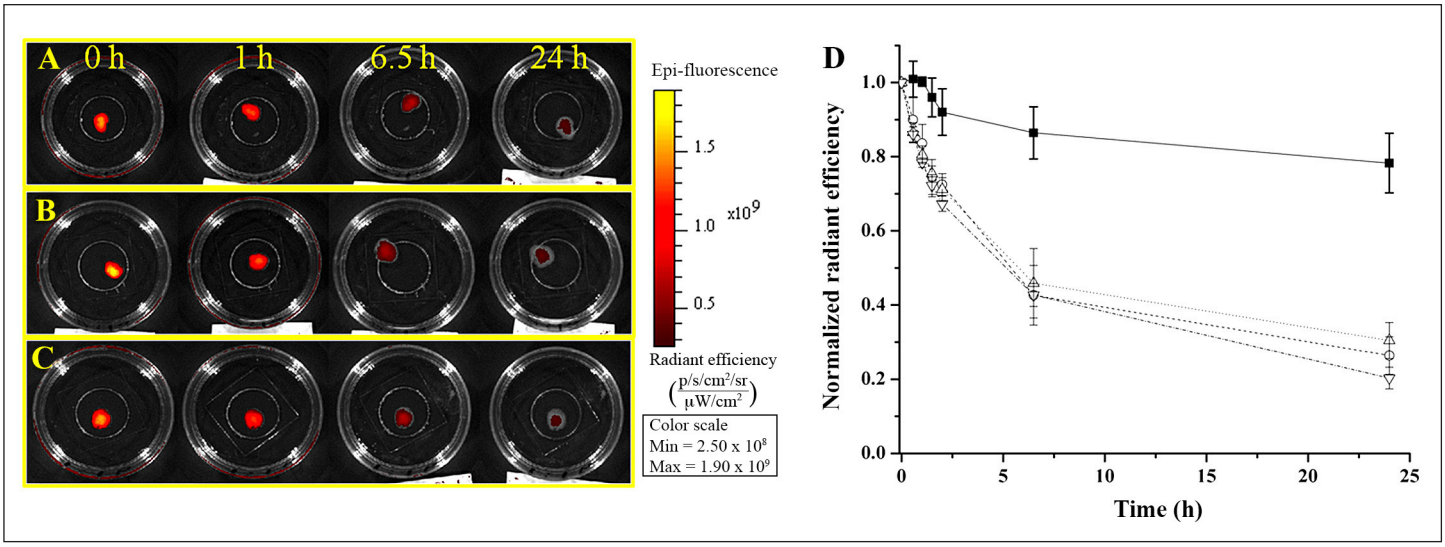

Figure 4. Gel 1 retention of glucose nanosensors. Fluorescent images of gel 1 with glucose nanosensors over time for **(A)** 5:1, **(B)** 2:1, and **(C)** 1:1 formulations of gel 1. **(D)** Normalized radiant efficiency of the gels over time for the bulk degradation control (—■—), 5:1 (--○--), 2:1 (···△···), and 1:1 (-·-▽-·-) formulations. n = 3 for all samples, and error bars represent standard deviations.

where A is the initial value, R_0 is the rate of decay, and t is time. The decay rates are displayed in **Table 3**. All three ratios of gel 1 had similar decay rates. Correspondingly, **Figure 5** shows the fluorescence decay of gel 2 ratios with encapsulated nanosensors over time. The total change in fluorescence signal and decay rates are less than gel 1 at the various ratios (**Table 3**). In the case of both gels, each formulation performed similarly except for their delayed response in the glucose permeability experiments. Therefore, 5:1 gel 1 and 5:1 gel 2 were selected for the *in vivo*

experiments because they had the shortest delays in responding to glucose.

In Vivo *Demonstration*

In vitro characterization of the gels demonstrated that gels can be used as an encapsulation vehicle for the glucose nanosensors *in vivo*. Mice were intradermally injected with 5:1 gel 1, 5:1 gel 2, and a no-gel control in three separate spots along the back (**Figure 6A**). Over the course of 1 h, the average normalized total radiant efficiency for three mice decreased to 14%, 41%, and 55% of the initial value for no gel, gel 1, and gel 2, respectively. For the first hour, the difference between the two gels and the control was significant ($p < .05$);

Table 3.
Decay Rates of the Average Total Radiant Efficiency over 6.5 h for Bulk Degradation Control and Each Formulation of Gel 1 and Gel 2

Condition	Decay rate (h^{-1})
Bulk degradation control	-0.02 ± 0.01
5:1 gel 1	-0.14 ± 0.03
2:1 gel 1	-0.12 ± 0.04
1:1 gel 1	-0.14 ± 0.02
5:1 gel 2	-0.08 ± 0.01
3:1 gel 2	-0.08 ± 0.01

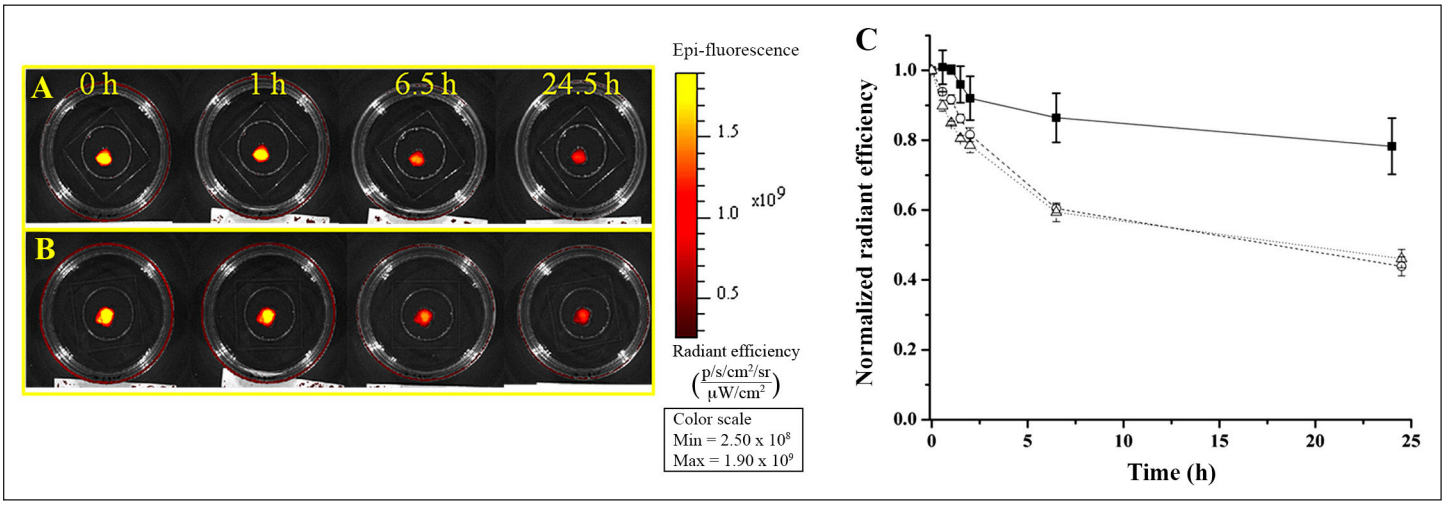

Figure 5. Gel 2 retention of glucose nanosensors. Fluorescent images of gel 2 with glucose nanosensors over time for **(A)** 5:1 and **(B)** 3:1 formulations of gel 2. **(C)** Normalized radiant efficiency of the gels over time for the bulk degradation control (—■—), 5:1 (--○--), and 3:1 (···△···) formulations. $n = 3$ for all samples, and error bars represent standard deviations.

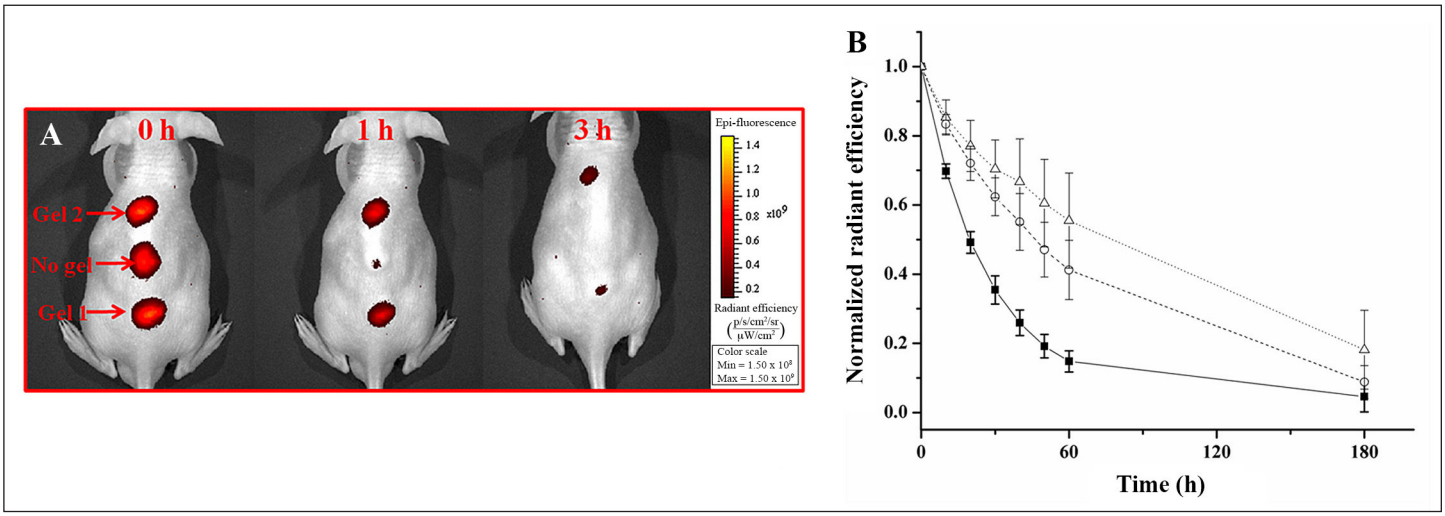

Figure 6. *In vivo* testing of nanosensors encapsulated in gel 1 and gel 2. **(A)** Fluorescent images of glucose nanosensors encapsulated in gel 1 and gel 2 along with a no-gel control over 3 h. **(B)** Normalized radiant efficiency of the gels over time for the no-gel control (—■—), gel 1 (--○--), and gel 2 (···△···). $n = 3$ for all samples, and error bars represent standard deviations.

however, there was no significant difference between gel 1 and gel 2 ($p > .05$). By 3 h, all three conditions had decreased to below 20% of the initial normalized efficiency, and there was no significant difference between all three conditions. The fluorescence of the sensors was completely diminished by 24 h (data not shown).

Discussion

Gel 1 and gel 2 were selected for these studies because they can be easily modified for stiffness through dilution,[18,19] and they are amenable to nanosensor incorporation during the gelling process. Three parameters were used to assess and downselect the optimal formulations for *in vivo* testing: encapsulation efficiency of the nanosensors, glucose permeability through the gel, and nanosensor retention within the gel over time.

The particles being suspended had the potential to inhibit gelation, as was noted with other matrices (data not shown). At several different formulations for gel 1 and gel 2, incorporating a sufficiently high concentration of nanosensors for *in vivo* detection into the pregelled components did not inhibit gelation. Additionally, since it is critical that implanted nanosensors can sense real-time changes in physiological concentrations of glucose even while in a gel, glucose permeability through the gel was assessed. Solute transport through hydrogels is governed by polymer chain mobility, charge groups, and solute versus pore size of the gel.[24] Gel 1 and gel 2 were permeable to glucose, and the shape of the kinetics of the fluorescence response of all the gels were similar to those reported by other groups on the transport of glucose through gels[21–23] such as calcium alginate.[21,22] This transport, as modeled using lag-time analysis, has an initial lag time followed by a linear increase in the amount of glucose that has passed through the gel. In our case, the lag time for glucose diffusion through the entire gel can overshadow one of the main advantages of using nanosensors: their fast response. The delays in response may be shortened by reducing the amount of gel to minimize the transport time to the center of the gel. However, these transport delays may be a major disadvantage for the use of a nanosensor/gel system to monitor real-time changes in glucose. Additionally, glucose gradients that may form throughout the gel could affect sensor measurements. Therefore, we are currently investigating the use of new sensing geometries that will increase the overall size of the sensors while retaining fast sensor response times and glucose transport.

Lastly, the diffusion of the nanosensors out of the gels was investigated to determine efficacy of sensor retention over time. The average size of the glucose nanosensors is 74 nm,[10] and gel pore sizes less than this would be desirable for greater retention. Reported values of pore size for gel 1 range from 26 nm to 2 μm for 1:1 dilution,[19,25] with pore size varying with gel 1 concentration.[19] Drastic changes in pore size of gel 1 was not evident from our results since all gel 1 formulations performed similarly, and we predict that the average pore size for these matrices was greater than the size of the nanosensors. On the other hand, gel 2 has been shown to retain proteins as small as 70 kDa.[18] The average pore size for gel 2 may be smaller than gel 1 and thus explains the greater retention of nanosensors over time.

Previous *in vivo* studies were limited to approximately 1 h because of loss of signal intensity at the injection site.[10] The majority of the signal loss was attributed to sensor diffusion from the point of injection. In our current work, immobilizing nanosensors in a gel matrix improved the lifetime to over 1 h *in vivo*; however, there was still a loss of signal over this time frame. Other factors such as sensor performance, photobleaching, and gel degradation contribute to loss of signal as well, and inclusion of a reference dye or internal standard into the sensors will help to normalize the loss of fluorescent signal to account for these effects on glucose measurements. Ultimately, the goal is a sensor that performs for at least one week *in vivo*, and this will require further improvements to the nanosensors and the injection techniques, in addition to the use of gels.

Conclusions

Two commercially available injectable gels sufficiently encapsulated glucose nanosensors while maintaining glucose permeability. Both gels prolonged sensor lifetime *in vivo* longer than nanosensors alone. However, more work will have to be done to improve nanosensor lifetime in order for them to be applicable for long-term diabetes monitoring.

Funding:

This work was funded by the IGERT Nanomedicine Science and Technology program at Northeastern University from National Cancer Institute and National Science Foundation grant DGE-0504331 and National Institutes of Health Grant 5RO1GM084366.

Acknowledgments:

We thank Kevin J. Cash and Ankita Shah for their technical guidance in preparing this article.

References:

1. U.S. Food and Drug Administration. P050012/S001. STS-7 Continuous Glucose Monitoring System. 2007. http://www.fda.gov/MedicalDevices/ProductsandMedicalProcedures/DeviceApprovalsandClearances/Recently-ApprovedDevices/ucm076983.htm.
2. U.S. Food and Drug Administration. P980022/S015. Paradigm REAL-Time and Guardian REAL-Time Systems. 2007. http://www.fda.gov/MedicalDevices/ProductsandMedicalProcedures/DeviceApprovalsandClearances/Recently-ApprovedDevices/ucm077026.htm.
3. Wang J. Electrochemical glucose biosensors. Chem Rev. 2008;108(2):814–25.
4. Pickup JC, Zhi ZL, Khan F, Saxl T, Birch DJ. Nanomedicine and its potential in diabetes research and practice. Diabetes Metab Res Rev. 2008;24(8):604–10.
5. Steiner MS, Duerkop A, Wolfbeis OS. Optical methods for sensing glucose. Chem Soc Rev. 2011;40(9):4805–39.
6. Cash KJ, Clark HA. Nanosensors and nanomaterials for monitoring glucose in diabetes. Trends Mol Med. 2010;16(12):584–93.
7. Chaudhary A, Harma H, Hanninen P, McShane MJ, Srivastava R. Glucose response of near-infrared alginate-based microsphere sensors under dynamic reversible conditions. Diabetes Technol Ther. 2011;13(8):827–35.
8. D'Auria S, Herman P, Rossi M, Lakowicz JR. The fluorescence emission of the apo-glucose oxidase from aspergillus niger as probe to estimate glucose concentrations. Biochem Biophys Res Commun. 1999;263(2):550–3.
9. Wang QS, Li GQ, Mao WY, Qi HX, Li GW. Glucose-responsive vesicular sensor based on boronic acid-glucose recognition in the ARS/PBA/DBBTAB covesicles. Sens Actuators B Chem. 2006;119(2):695–700.
10. Billingsley K, Balaconis MK, Dubach JM, Zhang N, Lim E, Francis KP, Clark HA. Fluorescent nano-optodes for glucose detection. Anal Chem. 2010;82(9):3707–13.
11. Balaconis MK, Billingsley K, Dubach MJ, Cash KJ, Clark HA. The design and development of fluorescent nano-optodes for in vivo glucose monitoring. J Diabetes Sci Technol. 2011;5(1):68–75.
12. Clark HA, Hoyer M, Philbert MA, Kopelman R. Optical nanosensors for chemical analysis inside single living cells. 1. Fabrication, characterization, and methods for intracellular delivery of PEBBLE sensors. Anal Chem. 1999;71(21):4831–6.
13. Dubach JM, Harjes DI, Clark HA. Fluorescent ion-selective nanosensors for intracellular analysis with improved lifetime and size. Nano Lett. 2007;7(6):1827–31.
14. Gopee NV, Roberts DW, Webb P, Cozart CR, Siitonen PH, Warbritton AR, Yu WW, Colvin VL, Walker NJ, Howard PC. Migration of intradermally injected quantum dots to sentinel organs in mice. Toxicol Sci. 2007;98(1):249–57.
15. Ozaydin-Ince G, Dubach JM, Gleason KK, Clark HA. Microworm optode sensors limit particle diffusion to enable in vivo measurements. Proc Natl Acad Sci U S A. 2011;108(7):2656–61.
16. Li Y, Rodrigues J, Tomás H. Injectable and biodegradable hydrogels: gelation, biodegradation and biomedical applications. Chem Soc Rev. 2012;41(6):2193–221.
17. Kleinman HK, Martin GR. Matrigel: basement membrane matrix with biological activity. Semin Cancer Biol. 2005;15(5):378–86.
18. Serban MA, Scott A, Prestwich GD. Use of hyaluronan-derived hydrogels for three-dimensional cell culture and tumor xenografts. Curr Protoc Cell Biol. 2008;Chapter 10:Unit 10.14.
19. Zaman MH, Trapani LM, Sieminski AL, Mackellar D, Gong H, Kamm RD, Wells A, Lauffenburger DA, Matsudaira P. Migration of tumor cells in 3D matrices is governed by matrix stiffness along with cell-matrix adhesion and proteolysis. Proc Natl Acad Sci U S A. 2006;103(29):10889–94.
20. Suckow MA, Danneman P, Brayton C. The laboratory mouse. Boca Raton: CRC Press; 2000.
21. Hannoun BJ, Stephanopoulos G. Diffusion coefficients of glucose and ethanol in cell-free and cell-occupied calcium alginate membranes. Biotechnol Bioeng. 1986;28(6):829–35.
22. Teixeira JA, Mota M, Venâncio A. Model identification and diffusion coefficients determination of glucose and malic acid in calcium alginate membranes. Chem Eng J Biochem Eng J. 1994;56(1):B9–14.
23. Wu DQ, Zhang GL, Shen C, Zhao Q, Li H, Meng Q. Evaluation of diffusion in gel entrapment cell culture within hollow fibers. World J Gastroenterol. 2005;11(11):1599–604.
24. Amsden B. Solute diffusion within hydrogels. Mechanisms and models. Macromolecules. 1998;31(23):8382–95.
25. Abrams GA, Goodman SL, Nealey PF, Franco M, Murphy CJ. Nanoscale topography of the basement membrane underlying the corneal epithelium of the rhesus macaque. Cell Tissue Res. 2000;299(1):39–46.